JOURNAL OF MECHANICS OF CONTINUA AND MATHEMATICAL SCIENCES
www.journalimcms.org

ISSN (Online) : 2454 -7190 Vol.-15, No.-1, January (2020) pp 1-18 ISSN (Print) 0973-8975

PERFORMANCE EVALUATION OF MULTIFOCUS COLOR IMAGE FUSION USING EXTENDED SPATIAL FREQUENCY AND WAVELET-BASED FOCUS MEASURES IN STATIONARY WAVELET TRANSFORM DOMAIN

N. Radha[1], T. Ranga Babu[2]

[1]Department of Electronics & Communication Engineering, Aditya Engineering College, Surampalem, Andhra Pradesh, India

[2]RVR & JC College of Engineering, Acharya Nagarjuna University, Guntur, Andhra Pradesh, India

[1]radha.nainavarapu@aec.edu.in, [2]trbaburvr@gmail.com

Corresponding Author: Nainavarapu Radha

Email: radha.nainavarapu@aec.edu.in

https://doi.org/10.26782/jmcms.2020.01.00001

Abstract

The Multifocus image fusion objective in visual sensor networks is to combine the multi-focused images of the same scene into a focused fused image with improved reliability and interpretation. However, the existing fusion methods based on focus measures are not able to get entire focused fused image since they neglect the diagonal neighbor pixels during the selection of the focused objects. In order to get an image with all objects in focus a novel image fusion method using extended spatial frequency and wavelet based focus measures in the stationary wavelet transform domain is proposed. In our method, initially the two multi-focus source images are transformed and decomposed as low and high-frequency sub bands by using stationary wavelet transform. Then, each sub band is divided into equal sub-blocks. Focused sub-blocks of low and high-frequency sub bands are selected by using the extended spatial frequency and wavelet based focus measures. Lastly, the fused image is restored by performing the inverse stationary wavelet transform on selected sub-blocks. The performance of the proposed method is verified by carrying out the fusion on artificial, natural and misregistered multifocus images. The results of the proposed method are then compared with the results of existing image fusion methods. The experimental results indicate that proposed method not only removes artifacts in the fused image due to the shift-invariance of stationary wavelet transform and also preserves sharp details using extended spatial frequency and wavelet based focus measures.

Keywords : Extended spatial frequency, focus measures, image fusion, wavelet-based focus measure

I. Introduction

In visual sensor networks, it became difficult to derive an image with all objects in focus due to the restricted depth of focus of optical lenses in camera sensors. The solution to this is a multi-focus image fusion, which combines multiple images of the same scene into a fused image which is more feasible for visualization and detection. Imagefusion can reduce redundancyand thus improve efficiency of transmission in visual sensor networks (VSN). Spatial and transform domain image fusion methodsare presented in the literature. However, spatial domain methods introduce undesirable effects such as image blurring and contrast reduction. To overcome these problems, multi-resolution fusion methods using Discrete Wavelet Transform (DWT) [XXIV], Multi-resolution Singular Value Decomposition (MSVD) [XI], Stationary Wavelet Transform (SWT)[X,XX], Discrete Cosine Harmonic Wavelet Transform (DCHWT) [VII], Lifting Stationary Wavelet Transform [VIII], Dual Tree Complex Wavelet Transform (DTCWT) [XVII], multi-scale transforms [XIII,XV,XVI,XVIII], signal processing techniques like spatial frequency [IX], statistical signal processing [I], and neural networks [XXX], have been developed by researchers.The DWT based fusion method had been verified to be an effective image fusion technique. However, DWT suffers from lack of shift–invariance because of the down-sampling process. The stationary wavelet transform (SWT) is one of the most precise ones excluding dearth of shift invariance caused by DWT and hence it is used for image fusion by many scholars. Further, a good fusion method not only relies on the transform but also depends on how to select the focused coefficients in the transform domain. Thus, focus measures [II, VI, XII, XIV, XXI-XXIII], are essential to select focused image areas from source images considered for fusion to get a sharper fused image. For multi-focus image fusion, numerous focus measures are available in the literature like variance, the Energy of Gradient (EOG), Spatial Frequency (SF), the Energy of Laplacian (EOL) and Sum Modified Laplacian (SML). These focus measures have been widely applied in the spatial and transform domain fusion algorithms. According to [VI], SML can afford better performance than SF, EOL and EOG. Xie, *et al*. in [XXVI] proved that Wavelet Based Focus Measure (WBFM) performs better than SML. In [V], the author considered variance as a focus measure of fusion. But, experiment results in [VI] show that variance provides inferior performance than other focus measures. Li, *et al*. in [IX] proposed Spatial Frequency (SF) based fusion in spatial domain. However, SF takes only vertical and horizontal neighbors into account during the selection of the focused pixels. Additionally, the diagonal neighbors could be included in the Extended Spatial Frequency (ESF) focus measure proposed by Zheng, *et al*. in [XXXII]. Sahoo, *et al*. in [XIX]proposed (DWT + Variance) variance based fusion in DWT domain. However, this method introduces artifacts due to shift variance of DWT. Liu Cao *et al.* in [III] proposed spatial frequency based fusion in Discrete Cosine Transform (DCT) Domain. But it introduces blocking effect due to DCT. In [XXIX], SML is considered as focus measure in SWT Domain (SWT+SML). From the literature, Extended Spatial Frequency and Wavelet Based Focus Measure have proven to be an effective focus measure for image fusion. Hence, the advantages of stationary wavelet transform in combination with ESF and WBFM focus measures are considered for multi-focus image fusion in this paper.

II. Preliminaries

Stationary wavelet transform

The DWT that is intensely sampled suffers from a dearth of shift invariance. To conquer this problem, SWT, which is shift-invariant and computationally efficient, was developed. Shift-invariance is realized by eliminating the down-sampling in the DWT. SWT is a multi-resolution transform with redundancy and shift invariance properties. These properties make it suitable for image fusion to create a high quality fused image.

The j^{th} level decomposition of 2D- SWT is implemented as given in Eq. (1):

$$\begin{aligned} cA_{j+1,k_1,k_2} &= \sum_{n_1}\sum_{n_2} F_0^{\uparrow 2^j}(n_1-2k_1)F_0^{\uparrow 2^j}(n_2-2k_2)cA_{j,n_1,n_2} \\ cD^h_{j+1,k_1,k_2} &= \sum_{n_1}\sum_{n_2} G_0^{\uparrow 2^j}(n_1-2k_1)F_0^{\uparrow 2^j}(n_2-2k_2)cA_{j,n_1,n_2} \\ cD^v_{j+1,k_1,k_2} &= \sum_{n_1}\sum_{n_2} F_0^{\uparrow 2^j}(n_1-2k_1)G_0^{\uparrow 2^j}(n_2-2k_2)cA_{j,n_1,n_2} \\ cD^d_{j+1,k_1,k_2} &= \sum_{n_1}\sum_{n_2} G_0^{\uparrow 2^j}(n_1-2k_1)G_0^{\uparrow 2^j}(n_2-2k_2)cA_{j,n_1,n_2} \end{aligned} \quad (1)$$

Where F_0 and G_0 are low and high pass decomposition filters.

Inverse 2D- SWT is implemented as given in Eq. (2):

$$cA_{j,n_1,n_2} = \frac{1}{4}\sum_{i=0}^{3}\begin{Bmatrix} \sum_{k_1}\sum_{k_2} F_1(n_1-2k_1-i)F_1(n_2-2k_2-i)cA_{j+1,k_1,k_2} \\ +\sum_{k_1}\sum_{k_2} G_1(n_1-2k_1-i)F_1(n_2-2k_2-i)cD^h_{j+1,k_1,k_2} \\ +\sum_{k_1}\sum_{k_2} F_1(n_1-2k_1-i)G_1(n_2-2k_2-i)cD^v_{j+1,k_1,k_2} \\ +\sum_{k_1}\sum_{k_2} G_1(n_1-2k_1-i)G_1(n_2-2k_2-i)cD^d_{j+1,k_1,k_2} \end{Bmatrix} \quad (2)$$

Where F_1 and $G_1$is low pass and high pass reconstruction filters.

Focus Measures

Focus measures are essential to estimate the focused areas from source images to get a sharper fused image for multifocus image fusion. The focus measure is maximum for focused areasin source images and minimum in defocusedareas. The focus measures used in the proposed method are described below:

Extended Spatial Frequency (ESF)

This focus measure estimates the clarity level of an image. High *ESF* results in high image resolution. The *ESF* comprises of row, column and diagonal frequencies. This spatial frequency includes diagonal information and thus results in extracting the fine details in an image. For an $N\times N$ image block $I(x, y)$ at position (x, y), the *ESF* is calculatedusing Eq. (3).

$$ESF = \sqrt{(RF)^2 + (CF)^2 + (MDF)^2 + (SDF)^2} \quad (3)$$

Where *RF* and *CF* are the row & column frequencies calculated using Eq. (4-5).

$$RF = \sqrt{\frac{1}{N\times N}\sum_{x=1}^{N}\sum_{y=2}^{N}[I(x,y) - I(x,y-1)]^2}\ , \tag{4}$$

$$CF = \sqrt{\frac{1}{N\times N}\sum_{x=1}^{N}\sum_{y=2}^{N}[I(x,y) - I(x-1,y)]^2}\ , \tag{5}$$

MDF and *SDF*- the main and secondary diagonal frequency calculated using Eq. (6-7)

$$MDF = \sqrt{\frac{1}{N\times N}\sum_{x=2}^{N}\sum_{y=2}^{N}[I(x,y) - I(x-1,y-1)]^2}\ , \tag{6}$$

$$SDF = \sqrt{\frac{1}{N\times N}\sum_{y=1}^{N}\sum_{x=2}^{N}[I(x,y) - I(x-1,y+1)]^2}\ , \tag{7}$$

Wavelet-based focus measure (WBFM):

Xie,*et al.*in [XXVI]proposed the wavelet-based focus measure based on discrete wavelet transform (DWT). In the DWTdomain, the energy of a focused image increases in high-frequency sub-bands and decreases in low-frequency sub-bands. For a defocused image, the energy, decrease in high-frequency subbands and increases in low-frequency subbands. Based on these properties wavelet-based focus measure is defined as in Eq. (8).

$$\emptyset = \frac{M_H^2}{M_L^2} \tag{8}$$

Where M_H and $M_L$are the high and low-frequency coefficientsof the DWT defined using Eq. (9-10):

$$M_H^2 = \sum_{I=1}^{K}\left[\sum_{(x,y)\in S_{LHI}} W_{LHI}^2(x,y) + \sum_{(x,y)\in S_{HLI}} W_{HLI}^2(x,y) + \sum_{(x,y)\in S_{HHI}} W_{HHI}^2(x,y)\right] \tag{9}$$

$$M_L^2 = \sum_{(x,y)\in S_{LL}} W_{LLK}^2(x,y) \tag{10}$$

Where *S* indicates a selected window operator whose equivalent windows operator in the level *I* sub-bands *LHI*, *HLI,* and *HHI* are designated S_{LHI}, S_{HLI}, S_{HHI}, respectively. W_{LHI}, W_{HLI}, *and* W_{HHI} are the high frequency coefficients in these sub bands. W_{LLK} is the low frequency coefficient of the K^{th}level. According to [XXVI], the coefficients of the first level DWT are used in (9) and the third level coefficients are used in (10).

III. Proposed Multifocus Image Fusion Algorithm

The proposed algorithm is implemented in steps as follows:

i. Consider two multi-focused source images (A & B) for fusion.

ii. For color images, transform source images in RGB color space to YCbCr color space.

iii. Compute one-level *SWT* on each Y- (intensity) component of color source images to obtain the low (LL) and high (LH, HL and HH) frequency sub bands. Divide each sub band into equal blocks of size 32 × 32.

iv. Fusion of low-frequency sub-bands:
The coefficients in the low-frequency sub-bands denote approximate information and hold more energy of the source images. However, the commonly used average based fusion rules for low frequency coefficients reduce the contrast of the fused image. It's verified that *ESF* reflects the clarity of an image. Hence, each block of LL sub band of fused image is calculated using Eq. (11):

$$LF_i = \begin{cases} LA_i, & if\ \ ESF_i^A \geq ESF_i^B \\ LB_i, & otherwise \end{cases} \quad (11)$$

Where ESF_i^A and ESF_i^B are the *ESF* of each block of LL sub band calculated using Eq. (3). LF_i represents the LL sub band of fused image.

v. Fusion of high-frequency sub-bands:
The coefficients in the high-frequency subbands denote detail information such as edges and salient features of the source images. However, the generally used absolute based fusion rules for high-frequency coefficients consider noisy pixels also. It's proven that the *WBFM* can well denote the salient features and sharp boundaries of an image. So, each block of high frequency sub band of fused image is calculated using Eq. (12):

$$HF_i = \begin{cases} HA_i, & if\ \ \emptyset_i^A \geq \emptyset_i^B \\ HB_i, & otherwise \end{cases} \quad (12)$$

Where Φi^A and Φ_i^B are the WBFM of each block of high frequency sub band calculated using Eq. (8). HF_i denotes the high frequency sub band of fused image. This step is implemented for all high frequency sub bands.

vi. Apply inverse *SWT* on each block of fused LL, LH, HL and HH sub bands to get fused image.

vii. Inverse transform fused image in YCbCr color space to RGB color space.

viii. Fused image quality is calculated in terms of reference and non- reference performancemeasures.

IV. Performance Evaluation

The proposed method performance can be evaluated using well known reference and non-reference measures.

Reference measures:

These measures are calculated based on the reference image.

Peak Signal to Noise Ratio (PSNR): It is an objective measure used to evaluate the quality of the fused image. The reference image is given by *R* and fused image is represented by *F*, *PSNR* is calculated using Eq. (13).

$$PSNR = 10\log_{10}\left[\frac{{P_{max}}^2}{\frac{1}{N\times N}[\sum_{x=1}^{N}\sum_{y=1}^{N}[R(x,y)-F(x,y)]^2]}\right] \quad (13)$$

Structural Similarity Index Measure (SSIM): SSIM[XXV]quantifies structuralsimilaritybetweentwoimages. The *SSIM* parameter on images *R* and *F* is calculated as in Eq. (14).

$$SSIM = \frac{(2\mu_R\mu_F+C_1)(2\sigma_{RF}+C_2)}{(\mu_R^2+\mu_F^2+C_1)(\sigma_R^2+\sigma_F^2+C_2)} \quad (14)$$

Feature Similarity Index Measure (FSIM): It is an image quality assessment measure proposed by Zhang, *et al*. [XXXI] and is defined using Eq. (15).

$$FSIM = \frac{\sum_{x,y\in\Omega} S_L(x,y)PC_m(x,y)}{\sum_{x,y\in\Omega} PC_m(x,y)} \quad (15)$$

Where Ω denotes the whole image

Non-Reference measures:

The calculation of these measures is not based on a reference image.

Mutual Information (MI): The *MI* is used for measuring the quality of fused image, and is defined using Eq. (16-18).

$$I_{AF}(F,A) = \sum p(F,A)\, log_2\left(\frac{p(F,A)}{p(F).p(A)}\right) \quad (16)$$

$$I_{BF}(F,B) = \sum p(F,B)\, log_2\left(\frac{p(F,B)}{p(F).p(B)}\right) \quad (17)$$

$$MI = I_{AF} + I_{BF} \quad (18)$$

Where $I_{AF}$and I_{BF}denote the normalized *MI* between the fused image (*F*) and the source images *A*&*B*.

Standard deviation (SD):*SD* is used for estimating the contrast of fused image. This is given by Eq. (19).

$$\sigma = \sqrt{\sum_{x=1}^{N}\sum_{y=1}^{N}(F(x,y)-\bar{F})^2}\,, \bar{F} = \frac{1}{NN}\sum_{x=1}^{N}\sum_{y=1}^{N}F(x,y) \quad (19)$$

Spatial Frequency (SF): To quantity the clearness of fused image, *SF* can be used .If the *SF* value is larger it denotes better fusion result and defined using Eq. (20-22).

$$RF = \sqrt{\frac{1}{N\times N}\sum_{x=1}^{N}\sum_{y=2}^{N}[F(x,y)-F(x,y-1)]^2} \quad (20)$$

$$CF = \sqrt{\frac{1}{N\times N}\sum_{x=1}^{N}\sum_{y=2}^{N}[F(x,y)-F(x-1,y)]^2} \quad (21)$$

$$SF = \sqrt{RF^2+CF^2} \quad (22)$$

Perceptual quality measure (Q_{CB}): Chen and Blum [IV], proposed Q_{CB} to measure the quality of fused image. Firstly, the global quality map Q_C is calculated.

$$Q_C(x,y) = \lambda_A(x,y)Q_{AF}(x,y) + \lambda_B(x,y)Q_{BF}(x,y) \quad (23)$$

$$Q_{CB} = \overline{Q_C(x,y)} \quad (24)$$

Q_{CB} is calculated by using Eq. (23-24).

Structural similarity-based measure (Q_Y): $Q_Y$proposed by Yang *et al.* [XXVIII] for fused image quality evaluation. Q_Y is given by Eq. (25).

$$Q_Y = \begin{cases} \lambda(w)SSIM(A,F|w) + \big(1-\lambda(w)SSIM(B,F|w)\big) \\ for\ SSIM(A,B|w) \geq 0.75 \\ \max\{SSIM(A,F|w), SSIM(B,F|w)\} \\ for\ SSIM(A,B|w) < 0.75 \end{cases} \quad (25)$$

Edge-preservationmeasure (Q_G): Xydeas and Petrovic [XXVII], proposed Q_G, which evaluates the amount of edge information conveyed from source images to fused image. Q_G is defined using Eq. (26).

$$Q_G = \frac{\sum_{x=1}^{N}\sum_{y=1}^{N} Q^{AF}(x,y)w^A(x,y) + Q^{BF}(x,y)w^B(x,y)}{\sum_{x=1}^{N}\sum_{y=1}^{N}\big(w^A(x,y)+w^B(x,y)\big)} \quad (26)$$

V. Experimental Results and Analysis

The proposed fusion method based on SWT and focus measures as well as existing fusion methods DWT, MSVD and SWT (with a decomposition level = 1), DTCWT (with a decomposition level = 4) DCHWT (with a decomposition level = 3),SF, DWT + Variance, SWT + SML have been experimented on Artificial, natural and misregistered multifocus images. All methods are implemented using MATLAB R2014a on a PC with 4 GB RAM, Intel core i3,3.70 GHz with Windows 10 Pro, 64 bits operating system.

i. Fusion of Artificial Multi-Focus Images

The first experiment is performed on artificially created images with divergent focus levels.

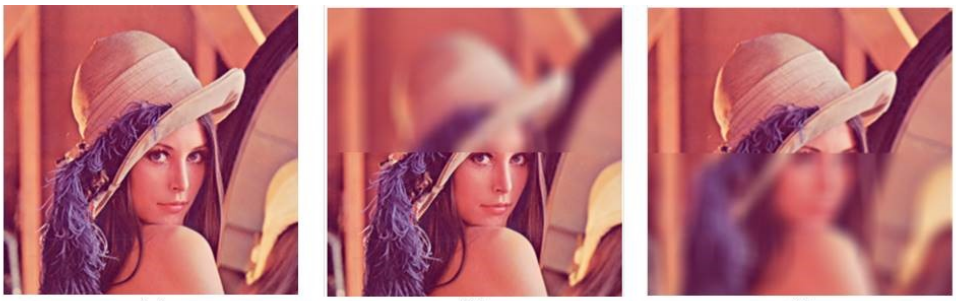

(a) (b) (c)

Fig 1 Reference and source images of Lena (a) Reference Image (b) Source image 1(blur on top) (c) Source image 2 (blur on down)

Fig 2 Comparison of fused images of different fusion methods (Lena): (a)-(i) Fused images using DWT [XXIV], MSVD [XI], SWT [X], DTCWT [XVII], DCHWT [VII], SF[IX] , DWT + Variance [XIX], SWT + SML [XXIX] and proposed method

The artificially blurred images were produced by filtering the reference image with a 15×15 Gaussian filter. One pair of color images of the Lenais considered for fusion. Both the reference and artificially generated source images of Lenaare shown in Figure 1. Fused images of Lenafrom different fusion methods are compared in Figure 2(a)-(i). The fused image quality is defined in terms of improved contrast, sharp details like edges and boundaries.

To evaluate the subjective assessment of various fusion methods, the zoomed images (which are sub images taken from the fused images) are considered as shown in Figure 3(a)-(i).

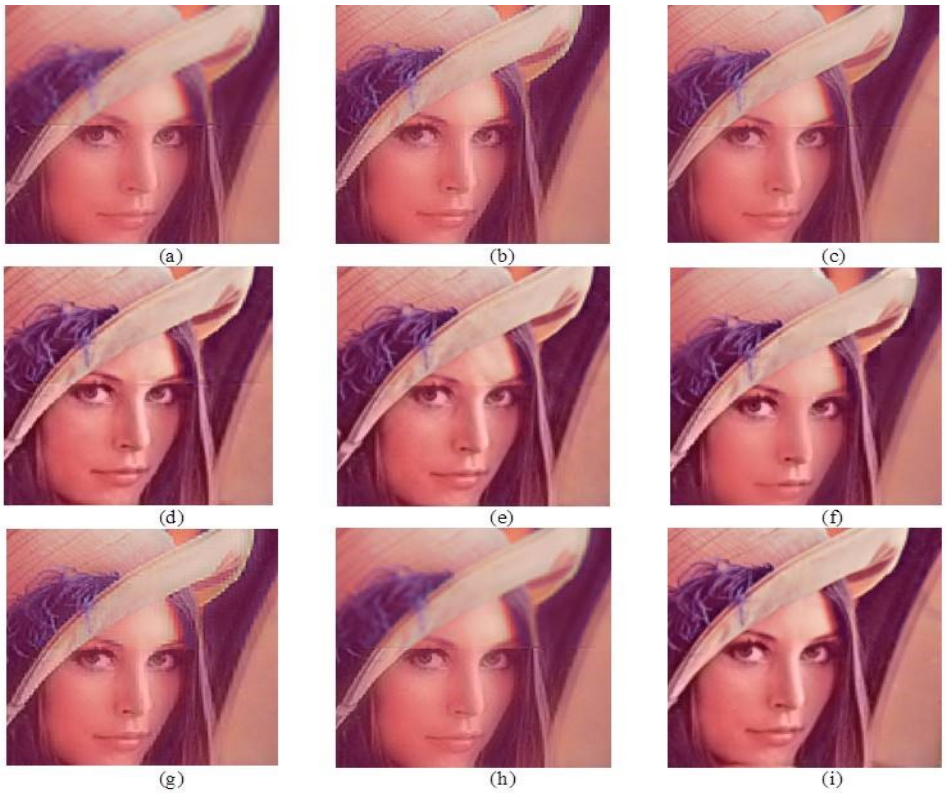

Fig 3 Comparison of zoomed images of different fusion methods (Lena): (a)-(i) zoomed images using DWT [XXIV], MSVD [XI], SWT [X], DTCWT [XVII], DCHWT [VII], SF[IX] , DWT + Variance [XIX], SWT + SML [XXIX] and proposed method

One can observe from Figure 3(a) that DWT [XXIV] method yields blurred effect as well as discontinuity at the border of divergent focus levels on the face of the Lenaand MSVD [XI] method in Figure 3(b) shows discontinuities at the edges. The SWT [X] method in Figure 3(c), DTCWT [XVII] method in Figure 3(d) and DCHWT [VII] method in Figure 3(e) also introduces edge discontinuities at the border of blurred and distinct regions. The SF [IX] method in Figure 3(f) shows blocking effect and DWT + Variance [XIX] method leads to artifacts at the face of Lena. SWT + SML [XXIX] in Figure 3(g) also show edge discontinuities at the border of blurred and distinct regions.

One can observe from Figure 3(i) that the proposed method gives the sub-image without blurring and good contrast. The logic is that the shift-invariance property of SWT in combination with ESF and wavelet based focus measures in the proposed method reduces artifacts with improved contrast and preserves edges more efficiently than other methods.

Table 1: Performance comparison based on reference and non-reference measures of variousfusionmethods

Artificial Multi-Focus Images	Fusion Method	Reference Measures			Non-Reference Measures					
		PSNR	SSIM	FSIM	MI	SD	SF	Q_{CB}	Q_Y	Q_G
Lena	DWT	27.1013	0.9701	0.9105	5.0907	54.6945	14.2013	0.5406	0.7005	0.3795
	MSVD	27.7903	0.9759	0.9335	5.0719	55.0437	16.5964	0.5369	0.7649	0.4239
	SWT	28.2727	0.9795	0.9374	5.1722	54.9652	15.4654	0.5624	0.7912	0.4454
	DTCWT	32.9903	0.9909	0.9880	5.2854	57.7759	19.6093	0.6624	0.8499	0.5124
	DCHWT	33.1908	0.9908	0.9888	5.4062	57.7855	18.7805	0.6354	0.8549	0.4961
	SF	29.9602	0.9850	0.9491	5.4122	56.7213	17.9604	0.5515	0.7922	0.4635
	DWT + Variance	27.9178	0.9770	0.9362	5.0569	55.1972	16.8174	0.5463	0.7589	0.4108
	SWT + SML	27.2163	0.9714	0.9115	5.1144	54.6658	13.8829	0.5399	0.7076	0.3886
	Proposed method	**33.8174**	**0.9915**	**0.9970**	**6.0299**	**58.7259**	**19.6446**	**0.7124**	**0.8960**	**0.5632**

The comparison of reference and non-reference measures of various fusion methods is given in Table 1. It can be observed from Table 1, PSNR, SSIM and FSIM are high inthe proposed method indicate that the quality of the fused image is better compared to other fusion methods. And also the proposed method has higher MI, SD and SF values compared to other methods. High MI value shows that the proposed method well transfers sharp details from source images to the fused image. A high SD and SF value shows that contrast and edges are preserved in the fused image. Q_{CB}, Q_Y, and $Q_G$are also high, indicating that the fused image of the proposed method will acquire good contrast, structural and edge information from the source images.

ii. Fusion of Natural Multi-Focus Images

The second experiment is performed on naturally obtained multifocus color images with divergent focus levels. One pair of color images of the children is considered for fusion. The source and the fused images of children are shown in Figure 4. To evaluate the fused image quality, the residual images are considered as shown in Figure 5. The residual images are the difference between the Y component of source and fused images. For focused areas, the difference between the source and fused images must be zero. In Fig. 5 (q) the area of fore ground and in Fig. 5 (r) the background part is entirely zero. This shows that the whole focused area is present in the fused image. But, the area of foreground as well as background part is also presented in the results attained by other methods shown in Fig. 5 (a) - (p).Hence, the proposed method well transfers focused details from source images and produce good contrast in the fused image. The logic is that the selection of focused low-frequency coefficients using extended spatial frequency and the selection of focused, high-frequency coefficients using wavelet based focus measures.

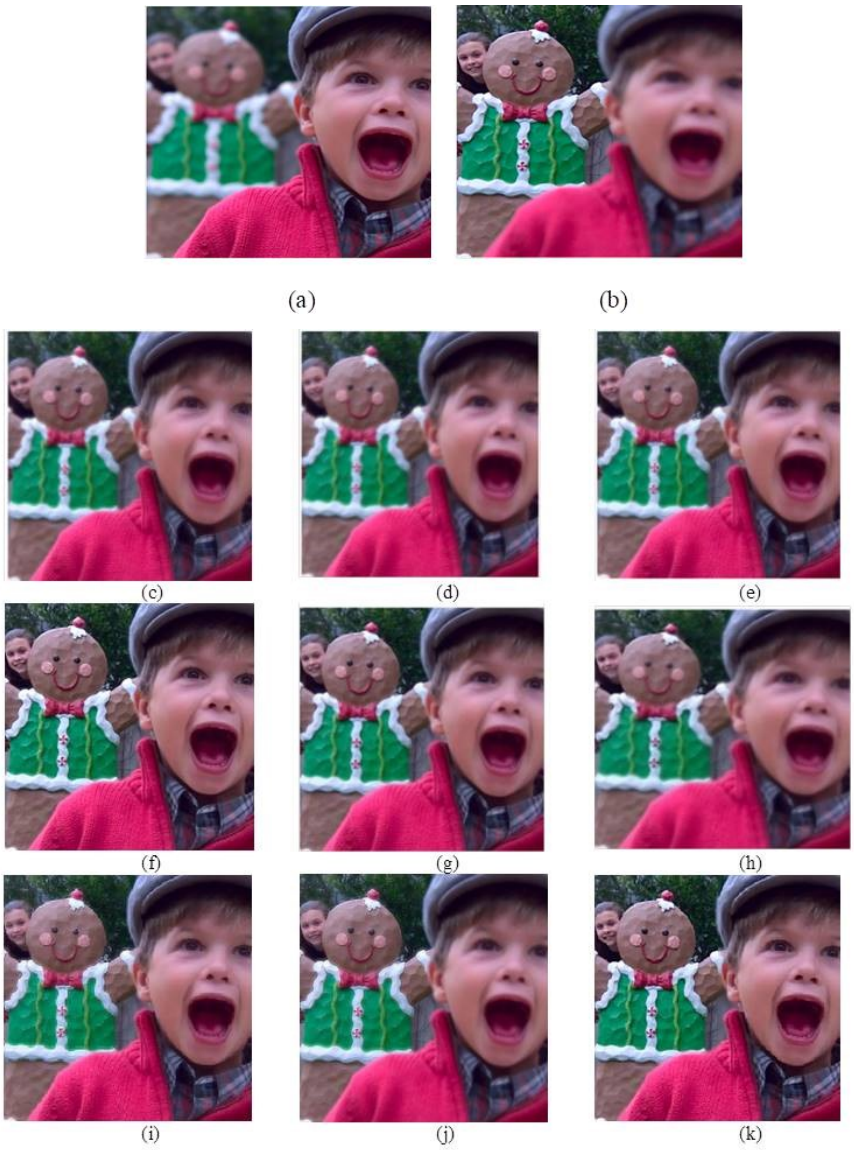

Fig 4 Source and fused images of Children: (a) Foreground Focused image (b) Background Focused image; (c)-(k) fused images using DWT [XXIV], MSVD [XI], SWT [X], DTCWT [XVII], DCHWT [VII], SF[IX] , DWT + Variance [XIX], SWT + SML [XXIX] and proposed method

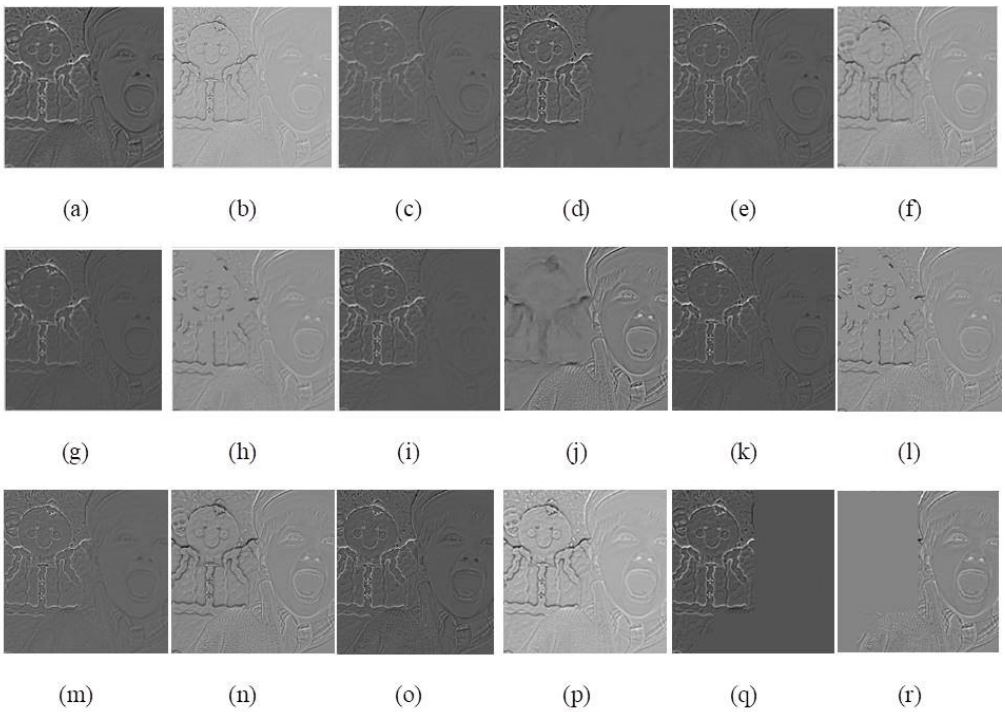

Fig 5 Difference image between figures: (a) 4 (a) and 4 (c); (b) 4(b) and 4(c); (c) 4(a) and 4 (d); (d) 4(b) and 4(d); (e) 4(a) and 4(e); (f) 4(b) and 4(e); (g) 4(a) and 4(f); (h) 4(b) and 4(f); (i) 4(a) and 4(g); (j) 4(b) and 4(g); (k) 4(a) and 4(h); (l) 4(b) and 4(h); (m) 4(a) and 4(i); (n) 4(b) and 4(i); (o) 4(a) and 4(j); (p) 4(b) and 4(j); (q) 4(a) and 4(k); (r) 4(b) and 4(k);

Table 2: Performance comparison based on non-reference measures of variousfusion methods

Natural Multi-Focus Images	Fusion Method	Non-Reference Measures					
		MI	SD	SF	Q_{CB}	Q_Y	Q_G
Children	DWT	6.2382	58.6170	15.0296	0.7090	0.8736	0.5602
	MSVD	6.0485	58.7137	17.6713	0.7056	0.8304	0.5568
	SWT	6.3828	59.0920	17.9889	0.7137	0.9230	0.6335
	DTCWT	6.2950	60.6955	21.6772	0.7248	0.9345	0.6237
	DCHWT	6.4796	59.6448	20.6123	0.7246	0.9376	0.6203
	SF	6.6459	59.1484	17.9372	0.7228	0.9013	0.6108
	DWT + Variance	6.1921	59.0807	18.8901	0.7028	0.9021	0.5788
	SWT + SML	6.4075	58.7598	16.4130	0.7095	0.8863	0.5715
	Proposed method	**6.9241**	**60.2023**	**21.5846**	**0.7516**	**0.9531**	**0.6516**

It is found from Table 2 that the proposed method has higher MI, SD, SF; Q_{CB}, Q_Y, and Q_G values compared to other fusion methods. This indicates that the proposed method well preserves sharp details in a fused image.

iii. Fusion of Misregistration Multi-Focus Images

Misregistration occurs in the multi-focus image set due to their diverse focal points or the movement of objects in the visual sensor Networks. Thus, the third experiment is performed on misregistration multifocus color images to assess the robustness of the proposed method. One pair of color images of the temple is considered for fusion. The source and experimental results of temple images are shown in Figure 6(a)-(k).

Fig 6 Source and fused images of Children: (a) Foreground Focused image (b) Background Focused image; (c)-(k) fused images using DWT [XXIV], MSVD [XI], SWT [X], DTCWT [XVII], DCHWT [VII], SF[IX] , DWT + Variance [XIX], SWT + SML [XXIX] and proposed method

Table 3: Performance comparison based on non-reference measures of variousfusionmethods

Misregistration Multi-Focus Images	Fusion Method	Non-Reference Measures					
		MI	SD	SF	Q_{CB}	Q_Y	Q_G
temple	DWT	3.1042	48.4896	20.0167	0.5482	0.7215	0.3680
	MSVD	3.1312	50.1462	28.6968	0.5618	0.8439	0.4803
	SWT	3.2651	49.9417	27.1434	0.5634	0.8701	0.5194
	DTCWT	3.0700	55.1996	32.8597	0.6298	0.9102	0.5673
	DCHWT	3.5849	51.7855	30.6000	0.6398	0.9341	0.5839
	SF	4.3200	51.9740	30.0197	0.6657	0.8911	0.5735
	DWT + Variance	3.0735	49.6694	28.3378	0.5526	0.8174	0.4468
	SWT + DCT + SML	3.2419	49.0397	23.6667	0.5496	0.8052	0.4306
	Proposed method	**5.3753**	**53.9722**	**31.9916**	**0.7375**	**0.9696**	**0.6474**

Although the source images of the Temple in Figure 6(a) and 6(b) are seriously misregistered due to the change of viewpoint, we can observe from Figure 6(k) that the boundaries and edges of the fused image are clear in the proposed method compared to other fusion methods.

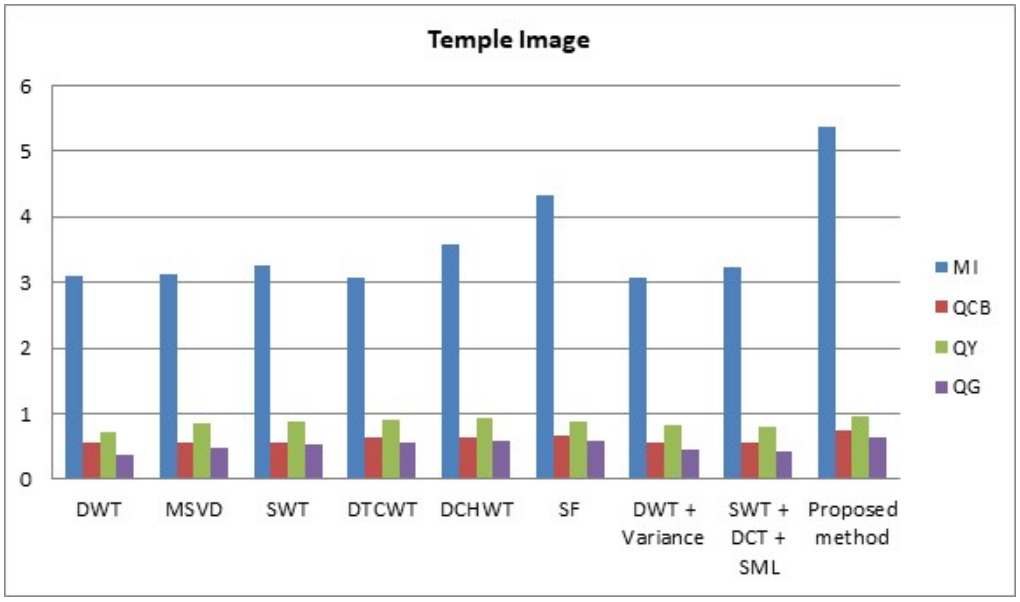

Fig 7 Comparison of MI, Q_{CB}, Q_Y, and Q_G

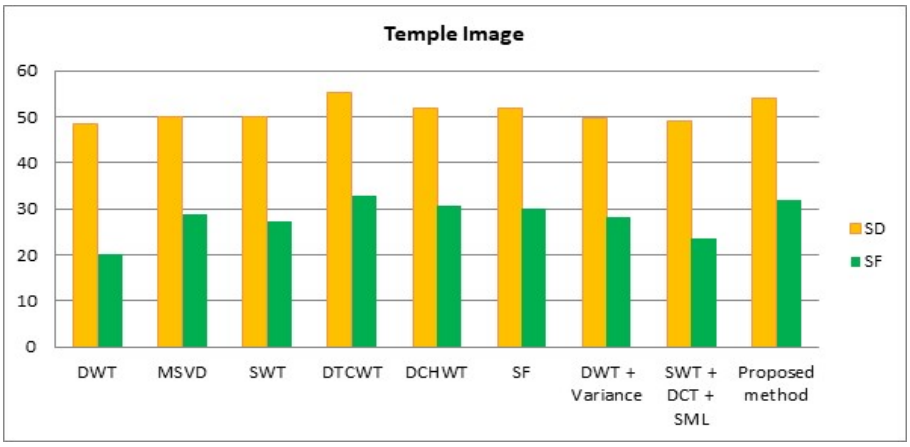

Fig 8 Comparison of SD, SF

Quantitative analysis of the proposed method of temple imageis done through non-reference measures like MI, SD, SF, Q_{CB}, Q_Y, and Q_G as given in Table 3.In Fig 7, the MI,Q_{CB}, Q_Y and Q_G of the proposed method are high Compared with the DWT, MSVD, SWT, DTCWT, DCHWT, SF, DWT + Varianceand SWT+SML methodsindicates that the sharp details from source images are transferred to fused image. In Fig 8, SD and SF values of the proposed method are also high compared to DWT, MSVD, SWT, and DCHWT methods shows that contrast and edges are preserved in a fused image. The SD and SF values of DTCWT are high compared to proposed method, but with a decomposition level of 4.

VI. Conclusion

In this paper, multi-focus image fusion using ExtendedSpatial Frequency and Wavelet Based Focus Measures in Stationary Wavelet Transform Domain has been developed. The shift-invariance property of Stationary Wavelet Transform makes the algorithm suitable for image fusion and help to produce a high quality fused image. And also the extended spatial frequency and wavelet based focus measures helps for effective selection of focused coefficients from low and high-frequency subbands in transform domain in order to get a focused fused image. The performance of the proposed fusion method is tested by applying the fusion on artificial, natural and misregistered multifocus images.Experimental results demonstrate that the proposed method preserves the image details in a far better way and extensively improves the fused image sharpness than other fusion methods. So our proposed fusion method is more suitable for visual sensor networks in the transmission of good quality fused images.

References

I. Bhatnagar G, Raman B. A new image fusion technique based on directive contrast. ELCVIA: electronic letters on computer vision and image analysis 2009;8(2):18-38.

II. Borwonwatanadelok P, Rattanapitak W, Udomhunsakul S. Multi-focus image fusion based on stationary wavelet transform and extended spatial frequency measurement. In: IEEE 2009 International Conference on Electronic Computer Technology, 2009 pp. 77-81.

III. Cao L, Jin L, Tao H, Li G, Zhuang Z, Zhang Y. Multi-focus image fusion based on spatial frequency in discrete cosine transform domain. IEEE signal processing letters 2014; 22(2):220-224.

IV. Chen Y, Blum RS. A new automated quality assessment algorithm for image fusion. Image and vision computing 2009; 27(10):1421-32.

V. Haghighat MB, Aghagolzadeh A, Seyedarabi H. Multi-focus image fusion for visual sensor networks in DCT domain. Computers & Electrical Engineering 2011; 37(5):789-97.

VI. Huang W, Jing Z. Evaluation of focus measures in multi-focus image fusion. Pattern recognition letters 2007; 28(4):493-500.

VII. Kumar BS. Multifocus and multispectral image fusion based on pixel significance using discrete cosine harmonic wavelet transform. Signal, Image and Video Processing 2013; 7(6):1125-1143.

VIII. Li H, Wei S, Chai Y. Multifocus image fusion scheme based on feature contrast in the lifting stationary wavelet domain. EURASIP Journal on Advances in Signal Processing 2012; 2012(1):39.

IX. Li S, Kwok JT, Wang Y. Combination of images with diverse focuses using the spatial frequency. Information fusion 2001; 2(3):169-176.

X. Li S, Yang B, Hu J. Performance comparison of different multi-resolution transforms for image fusion. Information Fusion 2011; 12(2):74-84.

XI. Naidu VP. Image fusion technique using multi-resolution singular value decomposition. Defence Science Journal 2011; 61(5):479-484.

XII. Nayar SK, Nakagawa Y. Shape from focus: An effective approach for rough surfaces. In: IEEE 1990 Robotics and Automation International Conference;Cincinnati,USA; 1990. pp. 218-225.

XIII. Paul S, Sevcenco IS, Agathoklis P. Multi-exposure and multi-focus image fusion in gradient domain. Journal of Circuits, Systems and Computers 2016; 25(10):1650123.

XIV. Pertuz S, Puig D, Garcia MA. Analysis of focus measure operators for shape-from-focus. Pattern Recognition 2013; 46(5):1415-1432.

XV. Petrovic VS, Xydeas CS. Gradient-based multiresolution image fusion. IEEE Transactions on Image processing 2004; 13(2):228-237.

XVI. Pu T, Ni G. Contrast-based image fusion using the discrete wavelet transform. Optical engineering 2000; 39(8):2075-2083.

XVII. Radha N, Babu TR. Performance evaluation of quarter shift dual tree complex wavelet transform based multifocus image fusion using fusion rules. International Journal of Electrical & Computer Engineering 2019; 9(2): 2377-2385.

XVIII. Sabre R, Wahyuni IS. Wavelet Decomposition in Laplacian Pyramid for Image Fusion. International Journal of Signal Processing Systems 2016; 4 (1): pp.37-44.

XIX. Sahoo T, Mohanty S, Sahu S. Multi-focus image fusion using variance based spatial domain and wavelet transform. In: IEEE 2011 International Conference on Multimedia, Signal Processing and Communication Technologies, 2011. pp. 48-51.

XX. Sharma EA, Gulati T. Performance Analysis of Unsupervised Change Detection Methods for Remotely Sensed Images. International Journal of Computational Intelligence Research 2017; 13(4):503-508.

XXI. Subbarao M, Tyan JK. Selecting the optimal focus measure for autofocusing and depth-from-focus. IEEE transactions on pattern analysis and machine intelligence 1998; 20(8):864-870.

XXII. Thelen A, Frey S, Hirsch S, Hering P. Improvements in shape-from-focus for holographic reconstructions with regard to focus operators, neighborhood-size, and height value interpolation. IEEE Transactions on Image Processing 2008; 18(1):151-157.

XXIII. Vadhi R, Kilari V, Samayamantula S. Uniform based approach for image fusion. In: Springer 2012 International Conference on Eco-friendly Computing and Communication Systems; Berlin, Heidelberg; 2012. pp. 186-194.

XXIV. Wang WW, Shui PL, Song GX. Multifocus image fusion in wavelet domain. In: IEEE 2003 Machine Learning and Cybernetics International Conference; Xi'an, China; 2003. pp. 2887-2890.

XXV. Wang Z, Bovik AC, Sheikh HR, Simoncelli EP. Image quality assessment: from error visibility to structural similarity. IEEE transactions on image processing 2004; 13(4):600-12.

XXVI. Xie H, Rong W, Sun L. Wavelet-based focus measure and 3-d surface reconstruction method for microscopy images. In: 2006 IEEE/RSJ International Conference on Intelligent Robots and Systems, 2006. pp. 229-234.

XXVII. Xydeas CA, Petrovic V. Objective image fusion performance measure. Electronics letters 2000; 36(4): 308-309.

XXVIII. Yang C, Zhang JQ, Wang XR, Liu X. A novel similarity based quality metric for image fusion. Information Fusion 2008; 9(2):156-60.

XXIX. Yang J, Ma Y, Yao W, Lu WT. A Spatial domain and frequency domain integrated approach to fusion multifocus images. The International Archives of the Photogrammetry, Remote Sensing and Spatial Information Sciences 2008; 37(PART B7).

XXX. Yang Y, Zheng W, Huang S. Effective multifocus image fusion based on HVS and BP neural network. The Scientific World Journal 2014.

XXXI. Zhang L, Zhang L, Mou X, Zhang D. FSIM: A feature similarity index for image quality assessment. IEEE transactions on Image Processing 2011; 20(8):2378-86.

XXXII. Zheng Y, Essock EA, Hansen BC, Haun AM. A new metric based on extended spatial frequency and its application to DWT based fusion algorithms. Information Fusion 2007; 8(2):177-192.